Numerical Modeling of Space Plasma Flows: ASTRONUM-2013
ASP Conference Series, Vol. 488
N. V. Pogorelov, E. Audit, and G. P. Zank, eds.

Improved Time Integration for WENO Methods in Astrophysical Applications

F. Kupka,[1] H. Grimm–Strele,[1] N. Happenhofer,[1] I. Higueras,[2] O. Koch,[3] and H.J. Muthsam[1]

[1]*Faculty of Mathematics, University of Vienna, Oskar–Morgenstern–Platz 1, A–1090 Wien, Austria*

[2]*Universidad Pública de Navarra, Departamento de Ingeniería Matemática e Informática, Campus de Arrosadia, 31006 Pamplona, Spain*

[3]*Vienna University of Technology, Institute for Analysis and Scientific Computing, Wiedner Hauptstraße 8–10, A–1040 Wien, Austria*

Abstract. Weighted essentially non-oscillatory methods are a powerful approach to discretize advection and pressure gradient terms in the hydrodynamical equations, since they yield higher effective resolution than traditional methods. But in some astrophysical problems, low Mach number flows have to be tackled or the flow may change from a low to a high Mach number flow, spatially or in time, and diffusion or radiative transfer can impose severe limitations on time steps allowed in explicit time integration methods. We provide a summary of new developments on semi-implicit time integration methods useful for astrophysical problems such as numerical simulations of stellar surfaces and envelopes, and the basic physical question of how to improve models of double–diffusive convection. We discuss several applications of these new methods.

1. Motivation

The numerical solution of the hydrodynamical equations may be subject to severely restricted maximum time steps imposed by source terms and by terms representing diffusion in the basic dynamical equations. This has motivated the development of new time integration methods discussed in the following. To do so we first introduce some definitions. Given a physical system and a set of dynamical equations $\mathrm{d}y(t)/\mathrm{d}t = f(y(t))$ describing its evolution in time, our intention is to compute an approximate solution as a function of time, i.e. we construct $Y_n = Y(t_n) \sim y(t_n)$ such that the numerical solution $Y(t)$ changes only by a few percent between t_n and t_{n+1}:

$$|Y_{n+1} - Y_n| < C\,|Y_n| \quad \text{with} \quad C \approx 0.05 \ldots 0.1. \tag{1}$$

This allows a sufficiently accurate propagation of the solution in time. Explicit time integration methods require to resolve the time dependence of all the processes described by the equations, independently of their amplitude and other properties:

$$|Y_{n+1} - Y_n| < D\,|Y_n| \quad \text{with} \quad D \ll C. \tag{2}$$

Implicit methods can be less restrictive and ideally achieve $D \approx C$ with $D \leqslant C$. In addition to numerical stability further properties such as positivity may be required. So,

how should one proceed? We motivate the methods discussed below with an example. For a two-species flow describing double-diffusive convection in planets or stars the Navier–Stokes and related conservation equations can be recast as

$$\underbrace{\frac{d}{dt}\begin{pmatrix}\rho\\ \rho c\\ \rho\boldsymbol{u}\\ e\end{pmatrix}}_{y'(t)} = \underbrace{-\nabla\cdot\begin{pmatrix}\rho\boldsymbol{u}\\ \rho c\boldsymbol{u}\\ \rho\boldsymbol{u}\otimes\boldsymbol{u}+P-\sigma\\ e\boldsymbol{u}+P\boldsymbol{u}-\boldsymbol{u}\cdot\sigma\end{pmatrix}-\begin{pmatrix}0\\ 0\\ \rho\mathbf{g}\\ \rho\mathbf{g}\cdot\boldsymbol{u}\end{pmatrix}}_{F(y(t))} + \underbrace{\nabla\cdot\begin{pmatrix}0\\ \rho\kappa_c\nabla c\\ 0\\ K\nabla T\end{pmatrix}}_{G(y(t))}. \tag{3}$$

Two terms related to diffusion have been split off here and collected in $G(y(t))$. The pressure terms P and $P\boldsymbol{u}$ may be separated as well (see Sect. 2, P is the product of the scalar pressure p with the unit tensor I). The same could be done for terms associated with momentum diffusion (the viscous stress tensor σ and $\boldsymbol{u}\cdot\sigma$).

We consider the numerical solution of (3) by a method of lines (MOL) approach: spatial derivatives are discretized by the fifth order weighted essentially non-oscillatory method developed by Jiang & Shu (1996) which achieves high accuracy for turbulent flows with shock fronts using a number of grid points affordable in astrophysical simulations (cf. Muthsam et al. 2010). After implementing proper boundary conditions a closed set of nonlinear, coupled ordinary differential equations (ODEs) is obtained.

case	$\Delta t_{\rm ad}$	$\Delta t_{\rm snd}$	$\Delta t_{\rm diff}$
convection (M dwarf)	7 s	0.52 s	383 s
semiconvection	19.47 s	2.45 s	3.72 s
Cepheid	2.31 s	1.73 s	0.057 s

Table 1. Time step limits in simulations of surface convection in an M dwarf and a Cepheid and a simulation of semiconvection (idealized, Prandtl number Pr = 0.1).

In Table 1 three astrophysical applications are collected which are modelled by (3) or its generalizations. For each the time step limitation by advection, $\Delta t_{\rm ad}$, is also the time scale on which the solution evolves. Ideally, the time step in the simulation would be 10% to 20% of this value. However, as is typical for a *low Mach number (Ma) flow*, the time step is limited by sound waves, $\Delta t_{\rm snd}$, for the M dwarf star, where Ma ~ 0.06. The simulation of a Cepheid type star is limited by *radiative diffusion* in layers just underneath the stellar surface (similar behaviour occurs in A-type stars, red giant, and AGB stars). The case of idealized semiconvection is more complex. Starting from a small perturbation, this is initially a low Mach number flow, but heat diffusion is almost equally restrictive until the layer becomes fully convective whence $\Delta t_{\rm ad} \sim \Delta t_{\rm snd}$.

In hydrodynamical problems there is often little gain from implicitly integrating the advection operator $\nabla\cdot(\rho\boldsymbol{u}\otimes\boldsymbol{u})$ and its counterparts $\nabla\cdot(\rho\boldsymbol{u})$, $\nabla\cdot(\rho c\boldsymbol{u})$, and $\nabla\cdot(e\boldsymbol{u})$ in time. If the time step Δt is limited by these terms, the solution $y(t)$ usually also changes on $t \sim \Delta t$. For $q > 1$, where q is the order of time integration, the important property of strong stability preservation is lost as soon as $\Delta t > 4\,\Delta t_{\rm ad}$ (cf. Kraaijevanger 1991; Ferracina & Spijker 2004, 2008; Ketcheson et al. 2009; Gottlieb et al. 2009).

On the other hand, if (3) is integrated in time with implicit-explicit Runge-Kutta (IMEX RK) methods, which integrate additive terms such as $F(y(t))$ and $G(y(t))$ by separate methods ($F(y(t))$ by an explicit method and $G(y(t))$ by an implicit one, for instance), generalized, linear or quasilinear Helmholtz equations are obtained which have

to be solved at each time step. However, these are scalar equations as opposed to the coupled system arising from a fully implicit integration of (3) and thus their solution is computationally much cheaper. The same occurs for the method of Kwatra et al. (2009) which allows a semi-implicit integration of terms containing ∇p (see Sect. 2). In both cases fast and well-converging methods are available for the generalized Helmholtz equations such as conjugate-gradient type methods and multigrid methods.

2. Kwatra's Method

Most methods for the solution of (3) are either only suitable for large Mach numbers (mean Ma $\gtrsim$ 0.3) or small ones (mean Ma $\lesssim$ 0.1). Kwatra et al. (2009) proposed an approach which yields accurate results from at least Ma $\sim$ 1 to Ma $\sim 10^{-3}$. They start from the fully compressible Navier–Stokes equations and associated conservation laws (3) and obtain an operator splitting method for the time integration of $\rho \boldsymbol{u}$ and e which requires to solve a generalized (linear) Helmholtz equation for intermediate values of the pressure. Happenhofer et al. (2013) provide a description of this algorithm when coupled to RK methods and how to modify it, if a buoyancy source term and diffusion terms are present. For IMEX RK methods it is embedded in the "explicit" part of the time integration. Tests performed by Kwatra et al. (2009), such as the 1D Sod shocktube, smooth high Mach number flows, and 2D circular shocks, can easily be reproduced. Happenhofer et al. (2013) also demonstrated that the Gresho vortex, an exact, stationary solution in 2D which can be constructed for arbitrary Mach numbers, is excellently preserved for $0.001 \leqslant \text{Ma} \leqslant 0.1$ while explicit time integration completely fails for Ma $\leqslant 0.01$ (see Fig. 1). Excellent scaling was demonstrated for simulations of double-diffusive convection in 2D on the VSC–2 cluster of the Vienna Universities.

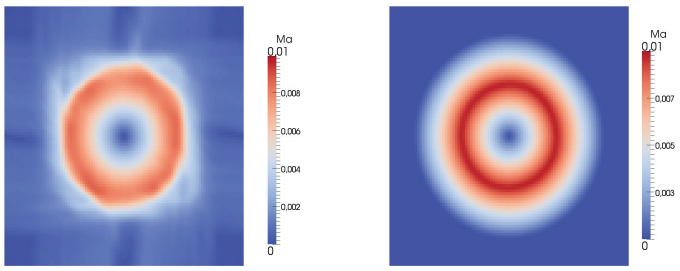

Figure 1. The Gresho vortex test for the fully explicit solver (left) and Kwatra's method (right) for a Mach number of Ma = 0.01 after a simulated time of 1.5 sec.

3. IMEX RK–methods and their applications

We consider a spatial discretization based on WENO methods (see Kupka et al. (2012); Happenhofer et al. (2013) for details) for (3) and the resulting ODE initial value problem $\dot{y}(t) = F(y(t)) + G(y(t))$, $y(0) = y_0$, where the vector fields F and G have different stiffness properties. An s-stage partitioned *Runge–Kutta (RK)* method, characterized

by coefficient matrices $A = (a_{i,j})$ and $\tilde{A} = (\tilde{a}_{i,j})$, proceeds from $y_{\rm old}$ to $y_{\rm new}$ as follows:

$$y_i = y_{\rm old} + \Delta t \sum_{j=1}^{s} a_{i,j} F(y_j) + \Delta t \sum_{j=1}^{s} \tilde{a}_{i,j} G(y_j), \quad i = 1, \ldots, s, \tag{4}$$

$$y_{\rm new} = y_{\rm old} + \Delta t \sum_{j=1}^{s} b_j F(y_j) + \Delta t \sum_{j=1}^{s} \tilde{b}_j G(y_j). \tag{5}$$

For IMEX RK methods $a_{i,j} = 0$ for $j \geq i$. Exact solutions may have properties such as monotonicity ($|y(t)| \leqslant |y(t_0)| \, \forall t \geqslant t_0$, with $|.|$ denoting some (semi-) norm), contractivity ($|y(t) - v(t)| \leqslant |y(t_0) - v(t_0)| \, \forall t \geqslant t_0$), boundedness ($m \leqslant y(t) \leqslant M$, if $m \leqslant y(t_0) \leqslant M \, \forall t \geqslant t_0$, which includes the special case of positivity with $m = 0$), and monotonicity of $y(t)$ with respect to $v(t)$ (where $y(t) \leqslant v(t)$, if $y(t_0) \leqslant v(t_0) \, \forall t \geqslant t_0$). If the exact solution is monotonic in this sense, the RK scheme should be monotonic as well. Numerical monotonicity can be ensured by strong stability preservation which means that $|Y_{ni}| \leqslant |y_n|$ for any stage i and internal stage solution Y_{ni} computed at time t_n, where finally also $|y_{n+1}| \leqslant |y_n|$. The maximum time step size for which this is possible is given through the *radius of absolute monotonicity* (Kraaijevanger 1991). A reformulation of RK schemes (Shu & Osher 1988) shows that a spatial discretization with a strong stability preserving RK scheme is monotonic in the above sense, if the monotonicity property holds already for the Euler forward scheme (usually only under some step size restrictions which depend on the radius of absolute monotonicity).

Higueras (2006) has developed a comprehensive theory of strong stability preserving (SSP) additive Runge–Kutta schemes where a *curve of absolute monotonicity* replaces the radius of absolute monotonicity. Step size restrictions are due to both F and G. This theory is applicable to the case of IMEX RK–methods. Not all combinations of SSP RK schemes yield SSP IMEX RK–schemes (Higueras 2006, 2009).

In Kupka et al. (2012), a variant of the SSP2(2,2,2) scheme as well as the modified SSP2(3,3,2) scheme from Higueras (2006) were applied to (3) for double-diffusive convection where a concentration gradient due to the heavier species counteracts a convective instability caused by a temperature gradient in a two-component flow. For the fully compressible case, Kwatra's method removes time step restrictions due to sound speed. Initially, the time step limitation is given by thermal diffusion which these IMEX methods improve by an order of magnitude compared to the fastest SSP RK explicit method (SSP(3,2) from Kraaijevanger 1991) applied to integrate the diffusion of concentration and heat in time. The importance of the SSP property was illustrated for the initial, diffusive phase (low fluid velocities, time step limited by diffusion) and the final advective phase of the simulations (high fluid velocities imposing a time step limit). In the model problem, the implicit integration of (3) just requires the solution of three linear, generalized Helmholtz equations (for concentration c, temperature T, and pressure p), as the diffusion terms in (3) remain linear. Thus, a solver based on a pre-conditioned conjugate gradient method parallelized using the Schur complement form of the linear equations (see Happenhofer et al. 2013) was sufficient to solve the systems of equations resulting from the (semi-)implicit time integration. These methods were all implemented into an improved version of the ANTARES code (Muthsam et al. 2010) which had originally been developed for radiation hydrodynamical simulations of stellar convection.

Once models for stars with realistic microphysics (equation of state, diffusivities, and other material properties) are considered, the generalized Helmholtz equations related to $G(y(t))$ become nonlinear. Mundprecht et al. (2013) presented numerical sim-

ulations with ANTARES in 2D for a Cepheid using a polar grid, spherically stretched and co-moving with mean pulsation velocity. For this case, Happenhofer (2013) has developed a solver for the nonlinear system of equations which results from solving the (radiative) diffusion term in (3) implicitly. Its nonlinearity originates from the fact that the heat diffusivity in a realistic fluid depends on T, ρ, and c. The IMEX approach assigns heat diffusion and its spatial discretization to $G(t)$ while all other terms in (3) are identified with $F(t)$ (no equation for c is used in this context).

For the Cepheid model discussed by Mundprecht et al. (2013) ($T_{\rm eff}$ = 5125 K, $\log(g) \sim 1.97$, $M = 5\,M_\odot$, thus $R \sim 38.5\,R_\odot$, and $L \sim 913\,L_\odot$, with an element mass fraction of $X = 0.7, Y = 0.29, Z = 0.01$), which has an approximate fundamental pulsational period of 3.85 d, and where roughly 42% of the outer part of the stellar radius is included in the computation, 1D models have been constructed by Happenhofer (2013). They assume spherical geometry with a grid of 454 points stretched along the radius by a factor q = 1.007. With closed boundaries ranging a mean T between 34000 K and 320000 K the best IMEX SSP RK–methods (particularly those discussed below) allow a time step only limited by advection and sound speed, about 100 times larger than the TVD2 method (Shu & Osher 1988) and more than 30 times larger than the fastest explicit method available to us, SSP(3,2). The speedup in wall-clock time reaches factors of 25 and 10, respectively: despite a much larger Δt the time steps of IMEX SSP RK–methods are only 3 to 4 times more expensive than those of explicit SSP methods.

One might wonder whether the SSP property is really needed for such flows. For a 2D simulation of semiconvection with 400×400 grid points Kupka et al. (2012) have investigated alternative IMEX schemes: the ARK3(2)4L[2]SA method by Kennedy & Carpenter (2003) is neither SSP for $F(y(t))$ nor $G(y(t))$ and never permitted time steps larger than those of explicit schemes. The original SSP2(3,3,2) scheme of Pareschi & Russo (2005), where the combination of two SSP schemes is only SSP in an asymptotic sense but not in the sense of Higueras (2006), permitted large timesteps in the diffusive phase, but failed in the advective phase. A third order non-SSP explicit RK method failed in 2D simulations of solar convection for which the TVD3 scheme (Shu & Osher 1988) worked. In a poster presented at this conference (M.A. Aloy, C. Aloy, S. Miranda Aranguren) it is reported that only the modified SSP2(3,3,2) scheme of Higueras (2006) works with the MCL limiter in a cylindrical MHD explosion test and permits a 3 to 4 times larger time step than the original scheme of Pareschi & Russo (2005) in a shock-tube test. The benefits from enhanced stability of SSP schemes thus appear to compensate for possibly smaller time steps.

4. New SSP IMEX RK–Methods and first results

The coefficients of RK schemes allow the construction of time integration methods with multiple properties instead of just maximizing the region of absolute monotonicity. Higueras et al. (2012) discuss a set of properties for IMEX RK–methods inspired by hydrodynamical simulations: if accuracy is limited by spatial resolution, it is sufficient to have a scheme which is second order in time with a small error constant. The scheme should be SSP and have a large region of absolute monotonicity. The stability function of the implicit scheme should tend to zero at infinity, its stability region containing a large subinterval of the negative real axis. This is ensured by requiring L-stability. For both schemes, the stability function g should be nonnegative for a large interval of the negative real axis. This prevents spurious oscillations of the numerical solution. Both

L-stability and positivity are implied by exact solutions of diffusion equations. Moreover, requiring uniform convergence in the sense of Boscarino (2008) guarantees higher than first order convergence also for arbitrarily stiff terms. For the explicit scheme, the stability region should contain large subintervals of the negative real axis and, optionally, also the imaginary axis may be inside that region, a requirement demanded for stable integration of the hyperbolic advection terms (Motamed et al. 2011, Wang & Spiteri 2007). The region of absolute monotonicity of the combined IMEX scheme should be large and for a convenient, memory-efficient implementation, the coefficients of the scheme should be rational numbers (to recombine the stages in a suitable way).

Higueras et al. (2012) have constructed several new SSP IMEX RK–methods which satisfy some or all of the aforementioned properties. In tests for the semiconvection problem (cf. Kupka et al. 2012) it has turned out that the two schemes which fulfil each of these properties or all but the inclusion of the imaginary axis in the stability region allow the largest time steps and also the shortest wallclock times (which depend heavily on the efficiency of the solver used for the implicit stage equation). The new SSP IMEX RK–methods may be useful for the numerical solution of any set of ordinary differential equations with mathematical properties similar to those obtained from spatial discretization of (3).

Acknowledgments. FK, HG, and NH are grateful for support through FWF grants P21742 and P25229. IH acknowledges support through the Ministerio de Ciencia e Innovación, project MTM2011–23203. The simulations have been run on the VSC-1 and VSC-2 clusters of the Vienna Universities.

References

Boscarino, S. 2008, SIAM J. Numer. Anal., 45, 1600
Ferracina, L., & Spijker, M. 2004, Math. Comp., 74, 201
— 2008, Appl. Numer. Math., 58, 1675
Gottlieb, S., Ketcheson, D., & Shu, C.-W. 2009, J. Sci. Comput., 38, 251
Happenhofer, N. 2013, Ph.D. thesis, University of Vienna
Happenhofer, N., Grimm-Strele, H., Kupka, F., Löw-Baselli, B., & Muthsam, H. 2013, J. Comput. Phys., 236, 96
Higueras, I. 2006, SIAM J. Numer. Anal., 44, 1735
— 2009, J. Sci. Comput., 39, 115
Higueras, I., Happenhofer, N., Koch, O., & Kupka, F. 2012, Optimized Imex Runge–Kutta methods for simulations in astrophysics: A detailed study, ASC Report 14, IASC, Vienna UT. http://www.asc.tuwien.ac.at/preprint/2012/asc14x2012.pdf
Jiang, G.-S., & Shu, C.-W. 1996, J. Comput. Phys., 126, 202
Kennedy, C., & Carpenter, M. 2003, Appl. Numer. Math., 44, 139
Ketcheson, D., Macdonald, C., & Gottlieb, S. 2009, Appl. Numer. Math., 59, 373
Kraaijevanger, J. 1991, BIT, 31, 482
Kupka, F., Happenhofer, N., Higueras, I., & Koch, O. 2012, J. Comput. Phys., 231, 3561
Kwatra, N., Su, J., Grétarsson, J., & Fedkiw, R. 2009, J. Comput. Phys., 228, 4146
Motamed, M., Macdonald, C., & Ruuth, S. 2011, J. Sci. Comput., 47, 127
Mundprecht, E., Muthsam, H., & Kupka, F. 2013, Mon. Not. Roy. Astron. Soc., 435, 3191
Muthsam, H., Kupka, F., Löw-Baselli, B., Obertscheider, C., Langer, M., & Lenz, P. 2010, New Astronomy, 15, 460
Pareschi, L., & Russo, G. 2005, J. Sci. Comput., 25, 129
Shu, C.-W., & Osher, S. 1988, J. Comput. Phys., 77, 439
Wang, R., & Spiteri, R. 2007, SIAM J. Numer. Anal., 45, 1871